A megaxion at 750 GeV as a first hint of low scale string theory

Luis E. Ibáñez and Víctor Martín-Lozano

Departamento de Física Teórica and Instituto de Física Teórica UAM/CSIC,
Universidad Autónoma de Madrid, Cantoblanco, 28049 Madrid, Spain

E-mail: luis.ibannez@uam.es, victor.martinlozano@uam.es

Abstract: Low scale string models naturally have axion-like pseudoscalars which couple directly to gluons and photons (but not W's) at tree level. We show how they typically get tree level masses in the presence of closed string fluxes , consistent with the axion discrete gauge symmetry, in a way akin of the axion monodromy of string inflation and relaxion models. We discuss the possibility that the hints for a resonance at 750 GeV recently reported at ATLAS and CMS could correspond to such a heavy axion state (*megaxion*). Adjusting the production rate and branching ratios suggest the string scale to be of order $M_s \simeq 7\text{--}10^4$ TeV, depending on the compactification geometry. If this interpretation was correct, one extra Z' gauge boson could be produced before reaching the string threshold at LHC and future colliders.

Contents

1   Introduction

ATLAS and CMS collaborations have recently reported hints of a 750 GeV resonance in the diphoton search [1, 2] for integrated luminosities of $3.2\,\text{fb}^{-1}$ and $2.6\,\text{fb}^{-1}$ respectively. The ATLAS collaboration presents an excess with a local significance of 3.6 σ while CMS collaboration obtained a local significance of 2.6 σ. These two statistical significances correspond to cross sections of $\sigma(pp \to \gamma\gamma) \sim 10.6\,\text{fb}$ (ATLAS) and $\sigma(pp \to \gamma\gamma) \sim 6.3\,\text{fb}$ (CMS). It is useful to compare these results to the diphoton searches in the first LHC run. The CMS diphoton search for a centre-of mass energy of $\sqrt{s} = 8\,\text{TeV}$ for an integrated luminosity of $19.7\,\text{fb}^{-1}$ reports a mild excess for a mass of 750 GeV with a cross section of $\sigma(pp \to \gamma\gamma) \sim 0.5\,\text{fb}$ [3], while ATLAS collaboration obtained $\sigma(pp \to \gamma\gamma) \sim 0.4\,\text{fb}$ for the same mass [4]. The 13 TeV data from ATLAS indicate a preferred value for the resonance width of $\Gamma = 45\,\text{GeV}$ [1] that supposes a not-so narrow width ($\Gamma/M \sim 6\%$). On the other hand CMS results suggest a better agreement with a narrow width, however when fitting the data they show that a width of $\Gamma = 42\,\text{GeV}$ is also compatible [2]. In that sense we can estimate that the resonance has an upper limit on its width of $\Gamma \lesssim 45\,\text{GeV}$. However both experimental observations are compatible with a narrow width and given the fact that the small resolution of the diphoton mass and the few number of events the resulting width could be overestimated.

One can also interpret this resonance as a particle and obtain information about it from the different experimental data. In that sense a pseudoscalar particle is highly motivated from the results reported by ATLAS and CMS. First of all the only allowed spins for a resonant particle decaying into two photons are 0 and 2 by the Landau-Yang theorem. Moreover if we compare the ratio between the cross sections at $\sqrt{s} = 8\,\text{TeV}$ and 13 TeV we obtain a factor of 5, this coincides with the gain factor of the production cross section of a (pseudo) scalar particle produced by gluons for those energies at a mass of 750 GeV [5]. However different searches at $\sqrt{s} = 8\,\text{TeV}$ present null results in searching for resonant production of particles decaying into Standard Model (SM) final states such as $t\bar{t}$ [6],

WW [7, 8], ZZ [8, 9], $Z\gamma$ [10], $\ell^+\ell^-$ [11, 12], $b\bar{b}$ [13]... Data seem to indicate that the pseudoscalar resonant particle only couples to gluons and photons. Several papers trying to disentangle the diphoton resonance in terms of axions or other different models could be found in refs. [14–127].

The effective Lagrangian of an axion η coupled to gluons and photons is

$$\mathcal{L}_{a_0} = \frac{\alpha_s}{4\pi} g_g \eta G_{\mu\nu} \widetilde{G}^{\mu\nu} + \frac{\alpha_{em}}{4\pi} g_\gamma \eta F^{em}_{\mu\nu} \widetilde{F}^{\mu\nu}_{em}, \tag{1.1}$$

where α_s and α_{em} are the strong and electromagnetic fine-structure constants, g_g and g_γ are model dependent constants. Axions η_i are related to their canonically normalised axions a_i by $\eta_i = a_i/f_i$, so that the kinetic term is

$$L_f = -\frac{1}{2}\partial_\mu a_i \partial^\mu a_i = -\frac{f_i^2}{2}\partial_\mu \eta_i \partial^\mu \eta_i . \tag{1.2}$$

and f_i are the corresponding axion decay constants. The couplings in eq. (1.1) are non-renormalizable and hence need some ultra-violet(UV) completion. In fact the corresponding completion is needed at a scale of order 10-100 TeV because otherwise unitarity would be violated in e.g. the gluon-gluon elastic scattering. Most of the models in the literature cure this problem by the introduction of new degrees of freedom which circulate in loops. It is important to remark that in our case the couplings in eq. (1.1) are tree level and unitarity would be restored due to the appearance of a new UV threshold corresponding to a low String Theory scale. As we will see, in order to match the data hints with an axion we will need parameters in the range $f/g_g \simeq 10^2$–10^3 GeV, $f/g_\gamma \simeq 1$–10^2 GeV. We also need an explanation as to why the axion does not couple to W's but it does couple to gluons and photons. And finally, we need an explanation as to how an axion-like object is so heavy, of order 750 GeV. Usual axions in particle physics are perturbatively massless and only acquire a mass due to non-perturbative potential. This potential is generated by instantons and is periodic under shifts $a_0 \to a_0 + 2\pi f$, which is an unbroken discrete gauge symmetry, and is the characteristic feature of an axion-like field.

It has been realised in the last few years that axion-like objects can get a perturbative mass term and still preserve the discrete shift symmetry if at the same time the parameters in the potential shift appropriately. These type of axions are sometimes called *monodromy axions*[128–133] and the simplest implementation of its symmetries is in terms of Minkowski 3-form fields $C_{\mu\nu\rho}$. Such 3-form fields do not propagate, since the corresponding equations of motion fix its field-strength to be constant, $F_{\mu\nu\rho\sigma} = \epsilon_{\mu\nu\rho\sigma} f_0$ [130–133]. The required structure is obtained from the following action [130, 131]

$$L = -\frac{1}{2}(\partial_\mu a_0)^2 - \frac{1}{2}|F_4|^2 + \mu a_0 F_4, \tag{1.3}$$

where $F_4 = \epsilon^{\mu\nu\rho\sigma} F_{\mu\nu\rho\sigma}$. Since the 3-form field has no propagating degrees of freedom in 4d, it behaves like an auxiliary field. Its equation of motion yields

$$F_4 = f_0 + \mu a_0 \tag{1.4}$$

leading to an induced scalar potential for the axion

$$V_a = \frac{1}{2}(f_0 + \mu a_0)^2. \tag{1.5}$$

This potential is invariant under the combined shift

$$a_0 \rightarrow a_0 + 2\pi f \quad f_0 \rightarrow f_0 - 2\pi\mu f . \tag{1.6}$$

As noted in [134, 135] the 4-form vev f_0 is quantized, and consistency with the symmetries requires $2\pi\mu f$ to be an integer in the same mass^2 units as f_0. Note that the axion a_0 has a mass $m_a = \mu$ and still the discrete shift symmetry is maintained. This class of monodromy axions have been recently considered in the context of string monodromy inflation [128–132] and more recently in the context of relaxion dynamics [136, 137].

The structure of the rest of the paper is as follows. In the next section we will show how a heavy axion with the couplings discussed above is compatible with the hints of a 750 GeV boson observed at CMS and ATLAS. In section (3) we will show how all the required ingredients are simultaneously present in string theory models with a string scale in the range 7–10^4 TeV. Once this work was finished refs. [126, 127] appeared (a few days or hours before our submission) which also consider the possibility of a string axion-like being the 750 GeV state.

2 A megaxion and the 750 GeV excess

A simple analysis of the cross section reported by ATLAS and CMS for 13 TeV [1, 2] gives us a central value of $\sigma_{\gamma\gamma} = 7.6 \pm 1.9$ fb, we will take this value in the rest of the paper. The production cross section of the axion decaying into two photons can be written as [125]

$$\sigma(pp \rightarrow a_0 \rightarrow \gamma\gamma) = \frac{C_{gg}}{\Gamma_{a_0} m_{a_0} s} \Gamma(a_0 \rightarrow gg)\Gamma(a_0 \rightarrow \gamma\gamma), \tag{2.1}$$

where we have used the narrow width approximation (NWA).[1] C_{gg} is the partonic integral for gluon production of the pseudoscalar, whose value for 13 TeV is $C_{gg}^{13\text{TeV}} = 2137$ [5]. The decay widths of the axion decaying into gluons and photons are

$$\Gamma(a_0 \rightarrow \gamma\gamma) = \kappa_\gamma^2 \frac{m_{a_0}^3}{64\pi}, \tag{2.2}$$

$$\Gamma(a_0 \rightarrow gg) = \kappa_g^2 \frac{m_{a_0}^3}{8\pi}. \tag{2.3}$$

Here we have defined

$$\kappa_i = \frac{\alpha_i}{4\pi}\frac{g_i}{f}, \quad i = g, \gamma. \tag{2.4}$$

We denote Γ_{a_0} to the total decay width of a_0 that is a sum over all possible decay channels of the pseudoscalar.

---

[1]We have assumed the NWA to obtain eq. (2.1). However as ATLAS collaboration reports the width of the resonance is compatible with a value of $\Gamma = 45$ GeV. In that case the error of taking this approximation is of the order of $\mathcal{O}(\Gamma/M) \sim 6\%$.

The axion can also decay into gluons in such a way that the dijet searches could be sensitive to it. The results of this search at $\sqrt{s} = 8\,\text{TeV}$ performed by ATLAS [138] and CMS [139] lead to an upper bound on the cross section of $\sigma_{jj} \lesssim 2.5$ pb for a mass of $750\,\text{GeV}$. In our case the dijet cross section is given by

$$\sigma(pp \to a_0 \to jj) = \frac{C_{gg}}{\Gamma_{a_0} m_{a_0} s} \Gamma(a_0 \to gg)^2. \tag{2.5}$$

It is clear from eq. (2.5) that this bound imposes a constant upper limit on κ_g if $\kappa_\gamma \ll \kappa_g$ and it becomes weaker as long as κ_γ grows.

In the same way one can consider photon production of the diphoton resonance given by,

$$\sigma(pp \to a_0 \to \gamma\gamma) = r_{\text{inel.}} \frac{C_{\gamma\gamma}}{\Gamma_{a_0} m_{a_0} s} \Gamma(a_0 \to \gamma\gamma)^2, \tag{2.6}$$

where $r_{\text{inel.}}$ is related with the number of protons that after radiating a photon get destroyed, and $C_{\gamma\gamma}$ is defined in the same way as C_{gg} but for photons. The values of these quantities are not well defined [140–142] Usually the values are given in the following ranges [140–142],

$$r_{\text{inel.}} \in [15 - 25], \quad R_{\gamma\gamma} = \frac{C_{\gamma\gamma}^{13\text{TeV}}/(13\text{TeV})^2}{C_{\gamma\gamma}^{8\text{TeV}}/(8\text{TeV})^2} \in [2 - 5]. \tag{2.7}$$

According to ref. [142] the preferred values are $r_{\text{inel.}} = 25$ that corresponds to the fact that only 4% of the protons survives to the collisions and $R_{\gamma\gamma} = 2.9$. However, in order to set constraints from the photon production we consider the most stringent values of this parameters that are $r_{\text{inel.}} = 25$ and $R_{\gamma\gamma} = 2$. The upper bound on the cross section given by the diphoton search at $\sqrt{s} = 8\,\text{TeV}$ of ATLAS and CMS is $\sigma_{\gamma\gamma} \lesssim 2.4$ fb [3, 4].

The results obtained are shown in figure (1) where we have plotted the diphoton cross section data in the plane $(\kappa_\gamma, \kappa_g)$ as a black dashed line and the green and yellow bands indicate the 1σ and 2σ values for this cross section. It is important to note that the dashed line together with the yellow and green bands are the only regions where the parameters fit the diphoton cross section. Out of this region the experimental results cannot be achieved. The vertical line for the cross section is given by the fact that the minimal value of κ_g to give the correct production of the axion is approximately of the order $10^{-5}\,\text{GeV}^{-1}$ and it is constant for any bigger value of κ_γ, since in that limit the decay width of the axion is mainly the decay width into photons, $\Gamma_{a_0} \approx \Gamma(a_0 \to \gamma\gamma)$. The horizontal line for the cross section can be understood in the same way as before changing κ_g by κ_γ and viceversa. For low values of κ_g, $(\kappa_g < 10^{-5}\,\text{GeV}^{-1})$ the observed cross section band is constant for κ_γ. This is because in that regime the diphoton cross section is achieved through photon production. The full black lines represent different values of κ_g and κ_γ giving decay widths for the axion of $45\,\text{GeV}$, $10\,\text{GeV}$, $1\,\text{GeV}$, $0.1\,\text{GeV}$, $0.01\,\text{GeV}$ for illustration. These lines only have physical meaning when the intersect with the regions allowed by the diphoton cross section i.e. the dashed line and the yellow and green bands. We take the line of $\Gamma = 45\,\text{GeV}$ as an upper limit on the decay width of the axion so the area above that line represents a greater value than the one given by ATLAS. In the whole manuscript we will consider as

valid points all the points that have a lower width that the one found by ATLAS, even if they are small. As it can be seen in figure (1) the decay width for the megaxion is always greater than $\Gamma > 10^{-3}\,\text{GeV}$. The blue region represents the exclusion region given by dijet searches at $\sqrt{s}=8\,\text{TeV}$ [138, 139]. For low values of κ_γ the exclusion limit is constant in κ_g since for those values the decay width of the axion is dominated by the decay into gluons. However when κ_γ grows to values greater than $10^{-3}\,\text{GeV}^{-1}$ the decay into photons becomes important so the dijet bound weakens. The red area corresponds to the exclusion region given by photon production [3, 4]. This area is constant to an approximate value $\kappa_\gamma = 3.5 \times 10^{-3}\,\text{GeV}^{-1}$, however this constraint becomes weaker when κ_g grows. If we want to explain the cross section given by the excess of $750\,\text{GeV}$, the dijet searches impose a bound on the maximum value of κ_g of approximately $\kappa_g \lesssim 3 \times 10^{-4}\,\text{GeV}$. On the other hand the maximum value for κ_γ is given by the photon production providing an upper limit of $\kappa_\gamma \lesssim 3.5 \times 10^{-4}\,\text{GeV}^{-1}$. The preferred value for the diphoton cross section provides three possible windows, one of this windows is the one with $\kappa_\gamma \simeq 3 \times 10^{-4}\,\text{GeV}^{-1}$ for values of $\kappa_g \lesssim 10^{-5}\,\text{GeV}^{-1}$ that corresponds to a width of the order of $\Gamma \simeq 10^{-1}\,\text{GeV}$. Another window is the one with $\kappa_g \simeq 8 \times 10^{-6}\,\text{GeV}^{-1}$ with $2 \times 10^{-5}\,\text{GeV}^{-1} \lesssim \kappa_\gamma \lesssim 3 \times 10^{-4}\,\text{GeV}^{-1}$ that covers widths between $\Gamma = 10^{-1}$–$10^{-2}\,\text{GeV}$. The other window corresponds to values of κ_γ that lie on the region $\kappa_\gamma \simeq 2.5 \times 10^{-5}\,\text{GeV}^{-1}$ for values of κ_g that lie in the region $8 \times 10^{-6}\,\text{GeV}^{-1} \lesssim \kappa_g \lesssim 3.5 \times 10^{-4}\,\text{GeV}^{-1}$ with widths from $\Gamma \simeq 10^{-2}\,\text{GeV}$ up to $\Gamma \simeq 1\,\text{GeV}$. Due to the exclusion given by dijet searches and photon production the maximun decay width of $\Gamma_{a_0} = 45\,\text{GeV}$ is not achieved in our scenario. We have also shown the areas constrained by ZZ and $Z\gamma$ searches at $8\,\text{TeV}$ [8–10] as violet and magenta regions. It is clear from figure (1) that the bounds imposed by those searches do not affect the signal cross section of the $750\,\text{GeV}$ resonance.

In figure (2) the diphoton cross section is depicted in the plane $(f/g_\gamma, f/g_g)$. As in the previous case the central value of the diphoton cross section is represented as a black dashed line and the 1σ and 2σ values are the green and yellow bands. The dijet exclusion area is represented as the blue region, and the ZZ and $Z\gamma$ exclusion areas are shown as violet and magenta regions. From this figure we can obtain the values of f/g_γ and f/g_g that reproduce the diphoton cross section divided in three different windows. The first one is for values in the region $20\,\text{GeV} \lesssim f/g_g \lesssim 10^3\,\text{GeV}$ and $f/g_\gamma \simeq 25\,\text{GeV}$, while the second one takes the values from the regions $2\,\text{GeV} \lesssim f/g_\gamma \lesssim 25\,\text{GeV}$ and $f/g_g \simeq 8 \times 10^2\,\text{GeV}$. The third region is given by $f/g_\gamma \simeq 2\,\text{GeV}$ for values of κ_g greater than $\kappa_g \gtrsim 10^3\,\text{GeV}$. If we consider that the values for g_g and g_γ are of order $\mathcal{O}(1)$ the values allowed for the axion decay constant are $1\,\text{GeV} \lesssim f \lesssim 10^3\text{GeV}$ in the whole allowed parameter space. It is important to note that for every allowed window the whole range of values for f may not be covered.

An important point here is the fact that if this excess is found to be correct, similar excesses are expected in the ZZ and $Z\gamma$ decay channels in future data, allowing a better reconstruction of the values of the parameters of the model.

In summary, an axion a_0 with couplings so constrained is consistent with the observed hints of a $750\,\text{GeV}$ boson. Such limits will in turn constraint the structure of possible low scale string models whose structure we discuss next.
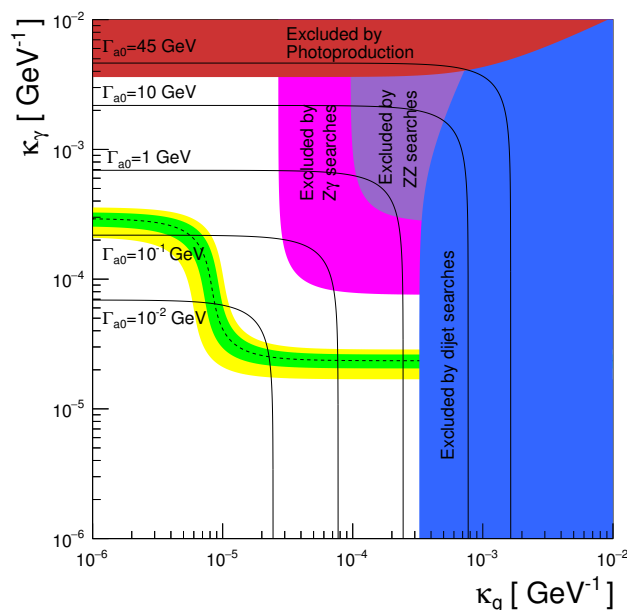
Figure 1. The effective coupling of the axion to photons κ_γ versus the effective coupling of the axion versus gluons κ_g. The central value of the cross section of the excess reported by ATLAS and CMS is shown as a black dashed line while the green and yellow bands indicate the 1σ and 2σ regions. The solid black lines represent different values of the axion decay width that are $\Gamma_{a_0} = 45, 10, 1, 0.1, 0.01$ GeV. The blue area defines the region excluded by dijet searches [138, 139], the violet and magenta areas are the regions excluded by ZZ and $Z\gamma$ searches respectively [8–10] while the red area is excluded by photon production [3, 4].

3   A megaxion at 750 GeV as a hint of low scale string theory

It is well known that the string theory scale may in principle be very low, even of order slightly above the EW scale, e.g. $M_s \simeq 7$–10^4 TeV [143] (see [144–149] for reviews). No sign of string resonances have been observed yet at LHC, indicating a lower bound for the string scale, e.g. $M_s \geq 7$ TeV [150]. In this scenario the fact that the Planck scale is much bigger than the string scale, $M_p \gg M_s$, is due to some extra dimensions (transverse to the branes in which the SM resides) being very large.

In what follows we will assume that the string scale is in the mentioned TeV range. We will mostly use for illustrative purposes a particularly interesting class of string models based on Type IIA orientifolds with intersecting branes [144–149], see the appendix. In these models the observable fermionic sector is that of the SM [151, 152]. The scheme of this large class of models is depicted in figure (3) . The quarks and leptons reside at the intersection of $D6$-branes which come in 4 stacks labeled a,b,c,d, and leading to a gauge group $\mathrm{U}(3)_a \times \mathrm{U}(2)_b \times \mathrm{U}(1)_c \times \mathrm{U}(1)_d$ respectively (the EW group may also be $\mathrm{Sp}(2) \approx \mathrm{SU}(2)$ if a single brane sits on top of the orientifold plane). The 4 stacks a,b,c,d of branes are called baryonic, weak, right and leptonic, because of the associated gauge symmetries. In addition to $\mathrm{SU}(3) \times \mathrm{SU}(2)$, the (visible) gauge group has thus up to 4 U(1)'s all of which get
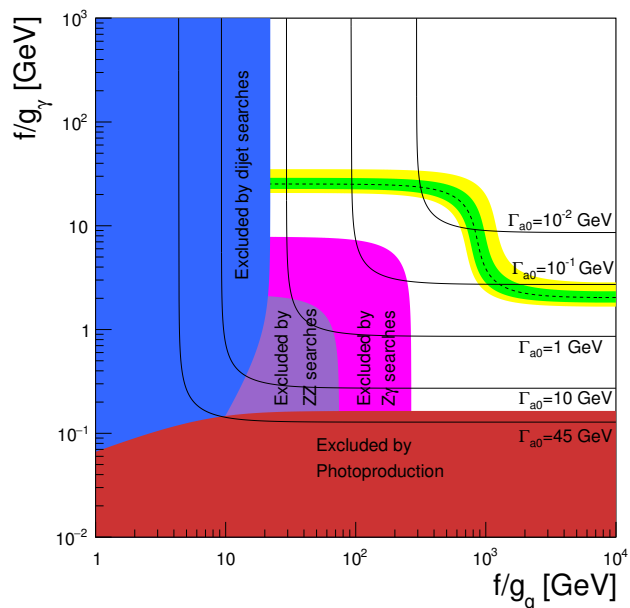
Figure 2. f/g_γ versus f/g_g. The central value of the cross section of the excess reported by ATLAS and CMS is shown as a black dashed line while the green and yellow bands indicate the 1σ and 2σ regions. The solid black lines represent different values of the axion decay width that are $\Gamma_{a_0} = 45, 10, 1, 0.1, 0.01$ GeV. The blue area defines the region excluded by dijet searches [138, 139], the violet and magenta areas are the regions excluded by ZZ and $Z\gamma$ searches respectively [8–10] while the red area is excluded by photon production [3, 4].
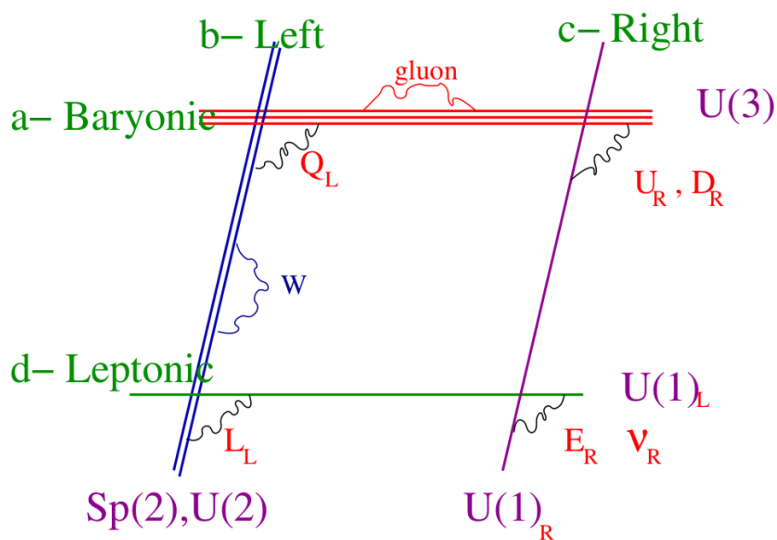
Figure 3. Quarks and leptons at intersecting branes.

a mass of order the string scale[2] by the Green-Schwarz mechanism except for hypercharge, which is a linear combination of the 4 U(1)'s. In particular one has

$$Q_Y = \frac{1}{6}Q_a - \frac{1}{2}Q_c + \frac{1}{2}Q_d \ . \tag{3.1}$$

In addition to the SM particles these models come along with scalar singlets coming from the closed string sector of the theory, the complex structure and Kahler moduli fields [151]. Among these there are always a set of axion-like fields coming from the Ramond-Ramond sector of the theory and in SUSY models become the imaginary part of the complex structure fields, $Im\, U_i = a_i$. They come from the dimensional reduction of RR 3-forms C_3 with legs in internal dimensions. In the toroidal setting there are 4 such scalars $i = 0, 1, 2, 3$ [151]. As we said, some of these would be axions get mass by combining with three linear combinations of the U(1)'s in the theory. To see how this happens it is more useful to consider an equivalent description of these axions in terms of 2-forms $B_i^{\mu\nu}$. They are related to the pseudo scalars by $\epsilon_{\mu\nu\rho\sigma}\partial^\sigma a_i = H_{\mu\nu\rho}^i$, where $H = dB$ is the field strength of each 2-form. There are then couplings [151]

$$c_i^\alpha \ B_i \wedge F_{U(1)}^\alpha \quad \alpha \ = \ a, b, c, d; \ i = 0, 1, 2, 3 \,, \tag{3.2}$$

where $F_{U(1)}^\alpha$ are the field strengths of the 4 U(1)'s. The coefficients c_i are integers in an appropriate normalisation. These couplings, when written in terms of the axions a_i are Higgs-like couplings which render massive all of the U(1)'s except for hypercharge. In particular one has couplings (see the appendix)

$$c_1^b \ B_1 \wedge F^b \tag{3.3}$$

$$c_2^d \ B_2 \wedge \ \left(-3F^a \ + \ F^d\right)$$

$$B_3 \wedge \ \left[c_3^a F^a \ + \ c_3^b F^b \ + \ \left(\frac{1}{3}c_3^a + c_3^d\right) F^c \ + \ c_3^d F^d\right] \ .$$

Note the important point that the 2-form B_0 (or its corresponding dual, the axion a_0) does not appear in any of these couplings and hence it does not combine with any gauge boson and remains massless at this level. This is more general than the toroidal setting. Generically there are axion fields like a_0 which have couplings to gauge bosons but are not the Goldstone boson of any U(1).

In addition to these couplings, the axions a_i have also axion-like couplings of the form

$$d_i^\alpha \ a_i(\text{tr}\ F_\alpha \wedge F_\alpha); \quad \alpha = a, b, c, d; \quad i = 0, 1, 2, 3 \ . \tag{3.4}$$

The d_i's are coefficients which are integers in an appropriate normalisation. Here F_α are the full U(n) field strengths of the 4 stacks. These couplings, combined with those in eq. (3.4) cancel all the residual mixed U(1) triangle anomalies of the massive U(1)'s. The massless axion a_0 has in general such couplings, with a general form

$$a_0 \ \left[d_0^a \ F^a \wedge F^a \ + \ d_0^b \ F^b \wedge F^b \ + \ d_0^d \ F^d \wedge F^d\right] \ . \tag{3.5}$$

---

[2]Or rather somewhat below, see [153, 154] and comments at the end of this section.

As we said, the coefficients d_0 are model dependent integers. In particular, as explained in the appendix, in a large class of models $d_0^b = 0$ and the unique massless axion will couple only to SU(3) and to hypercharge (via U(1)$_a$ and U(1)$_d$, which do couple to a_0). In the class of toroidal models discussed in the appendix this happens when one has an integer $n_b^1 = 0$. Thus we are left with axion couplings of the general form discussed in the introduction, i.e.

$$\mathcal{L}_{a_0} = \frac{\alpha_s}{4\pi} g_g \frac{a_0}{f} G_{\mu\nu} \widetilde{G}^{\mu\nu} + \frac{\alpha_Y}{4\pi} g_Y \frac{a_0}{f} B_{\mu\nu} \widetilde{B}^{\mu\nu}, \tag{3.6}$$

Note that the dependence on the couplings α_s, α_Y arises once one sets the gauge kinetic terms $F^2/(4g^2)$ to canonical form, whereas g_g, g_Y are model dependent constant coefficients. In the case of the QCD coupling g_g is proportional to the d_0^a coefficient. However, in the case of hypercharge it will be connected to both d_0^a and d_0^d, since both U(1)^a and U(1)^d appear in the definition of hypercharge, see eq. (3.1). Furthermore, in the case of hypercharge several branes are involved and the geometric factors ξ (see below) will in general affect differently the different branes. The upshot is that g_g/f and g_Y/f should be considered independent parameters, to be fixed by experiment. This is what we have done in the phenomenological analysis in the previous section.

In summary this class of Type IIA orientifold models generically has a single axion-like field a_0 which remains light after the U(1)'s other than hypercharge get a mass. Morover, there are large classes of models in which this axion has couplings to gluons and hypercharge but not to SU(2) gauge bosons. It is remarkable that these conditions, required by experimental data, appear in the model so neatly.

The size of the axion couplings to gluons and photons is controlled by the value of the axion decay constant f, which in this class of models should be controlled in turn by the string scale M_s. As we said, in models with a low string scale one needs dimensions transverse to the SM branes to become very large, to understand why $M_p \gg M_s$. This cannot be achieved in a purely toroidal model with intersecting D6-branes, because then some or all of the gauge couplings become negligibly small.[3] Still it is feasible in other generic CY compactifications in which the SM D6-branes wrap only a local region of the compactification in which volumes are not large. We can make a heuristic estimate of the relationship between the decay constant f and the string scale as follows. The kinetic term of the axion field η may be written as

$$\frac{M_p^2}{8\pi(S + S^*)} \partial_\mu(\frac{\eta}{8\pi^2}) \partial^\mu(\frac{\eta}{8\pi^2}) \tag{3.7}$$

where $Re\, S$ is the scalar partner of a_0. One can estimate the value of $Re\, S$ by recalling that the gauge coupling associated to SU(3) is approximately given by

$$(S + S^*) \simeq \frac{g_3^2}{2\pi} = \frac{g_s V_\Pi^{-1}}{2\pi M_s^3}, \tag{3.8}$$

---

[3]There are intersecting D5-brane toroidal models at singularities in which one can safely take two transverse directions very large still maintaining gauge coupling constants of observed size [152]. We have preferred not to use these models here as examples since their description is slightly more technical. For those the geometrical parameters ξ mentioned below are of order one.

where V_Π is the volume of the 3-cycle wrapped by the D6's associated to the SU(3) group, g_s is the string coupling and $M_s = (\alpha')^{-1/2}$ is the string scale. Taking into account that

$$M_p^2 \;=\; \frac{8V_6}{g_s^2(2\pi)^6\alpha^4} \tag{3.9}$$

one obtains for the axion decay constant

$$f \;\simeq\; \frac{M_s}{(2\pi)^{13/2}}\xi \;\simeq\; \xi \times 10^{-5}M_s\,, \tag{3.10}$$

Here ξ is a geometric factor, which in the toroidal case is $\xi = (V_6/V_\Pi^2)^{1/2}$, but one expects $\xi \simeq 1$ for more realistic models in which the SM is localised in a CY region with volumes not too different from the string scale. So one expects the decay constant f to be well below the string scale. Let us however emphasise that the precise evaluation of f within a given realistic model would require details about the geometry of the compactification and how all the moduli are fixed. The message here is that one has $f \ll M_s$ and hence a value of $f \simeq 10^2$–10^3 GeV is not in contradiction with the LHC bounds yielding $M_s \gtrsim 7$ TeV. Let us finally note that the fact that f is well below M_s in localised brane models can be shown in other contexts, see the Type IIB example below.

Up to now we have not discussed how the axion a_0 gets a large mass, possibly of order 750 GeV. As we said above, it would be very attractive if the axion a_0 here discussed had a monodromy structure so that a 4-form exists which can induce a non-trivial potential and an axion mass. In Type IIA orientifolds of the type in our example such couplings do exist. The 10D action contains couplings of the form (see e.g. [144])

$$S_{IIA} \;\propto\; -\int_{10D}(|F_4|^2 \;+\; F_4 \wedge H_3 \wedge C_3 \;+\; \ldots)\,. \tag{3.11}$$

Here F_4 is the field strength of the Type IIA 3-form $C_{\mu\nu\rho}$ with indices in Minkowski space and H_3 is the (quantized) flux associated to the Neveu-Schwarz 2-form B_2 with indices in compact dimensions. Expanding C_3 and H_3 in terms of harmonic 3-forms basis (α_j, β^i) [155–159]

$$H_3 = \sum_i H_i\beta^i, \quad C_3 = \sum_j \eta_j\alpha_j, \quad \int_{CY} \alpha_j \wedge \beta^i = \delta_j^i\,, \tag{3.12}$$

one obtains the structure

$$S_{a_i} \;\propto\; -(|F_4|^2 \;+\; F_4 H^i a_i)\,. \tag{3.13}$$

Using the equations of motion for F_4 and allowing the latter to have a quantized value one has an $\eta_i = a_i/(2\pi f_i)$ axion potential of the form

$$V \;=\; \sigma f^4|n_0 - \sum_i h_i\eta_i|^2\,, \; n_0, h_i \in \mathbf{Z}\,, \tag{3.14}$$

where on dimensional grounds we have set the overall scale of order f^4, with σ a model dependent fudge factor. Upon discrete shifts $a_i \to a_i + 2\pi f_i$, the potential remains invariant

with a shift $n_0 \to n_0 + h_i$. We see that in the case of the axion a_0 considered in the above example, one finds an axion mass given by

$$m_{a_0}^2 \;=\; \sigma f^2 h_0^2 \;. \tag{3.15}$$

The precise value is controlled by the model-dependent geometrical factor σ and the quantized NS flux h_0. However one expects that axion masses of order f to be natural.

Both facts, having axions coupling to QCD and hypercharge, not getting a Stuckelberg mass, but getting a mass instead through fluxes is not a particular property of Type IIA orientifolds but seems to be present more generally in string compactifications with a low string scale. Let us briefly describe how similar ingredients seem to arise in a class of Type IIB orientifold models with a compact CY manifold with *swiss cheese* structure [160, 161]. These are Type IIB models with a large volume structure (see [162] for an introduction and references). In the simplest canonical models of this class one has two complex Kahler moduli T_b and T_s with real parts τ_b, τ_s and $\tau_b \gg \tau_s$. The Kahler potential has a structure

$$\kappa_4^2 K \;=\; -2\log(\tau_b^{3/2} \;-\; \tau_s^{3/2}) \;\simeq\; -3\log(\tau_b) \;+\; 2\left(\frac{\tau_s}{\tau_b}\right)^{3/2} \tag{3.16}$$

Let us assume that the SM is realised through a local set of intersecting D7-branes in which the three branes corresponding to QCD are wrapping a 4-cycle with volume parametrized by the small modulus τ_s. The rest of the SM gauge interactions will be assumed to reside in other (intersecting) 4-cycles. Thus we have a U(3) gauge kinetic function $f_{U(3)} = T_s/2\pi$. The hypercharge generator here will contain the U(1) inside U(3), so that the axion $Im\,T_s$ will couple both to QCD and hypercharge, but in principle not to SU(2). We will also assume that $Im\,T_s$ does not get a mass from a Stuckelberg coupling, something which is a model dependent issue. Then it is an easy exercise to compute what is the size of the axion decay constant. One finds

$$f \;=\; \left(\frac{3}{32\pi}\right)^{1/2} \frac{1}{(\tau_s \tau_b^3)^{1/4}} \frac{M_p}{8\pi^2} \;=\; \left(\frac{9\alpha_{U(3)}}{\pi^2 g_s}\right)^{1/4} \frac{M_s}{16\pi^2} \;. \tag{3.17}$$

Taking $\alpha_{U(3)} \simeq g_s \simeq 0.1$, one obtains $f \simeq 5 \times 10^{-3} M_s$. Thus again the axion decay constant is well below the string scale, as in the Type IIA case discussed above.

In this case the mass of the axion will not arise from standard closed string fluxes, which in Type IIB orientifolds only give masses to the complex structure and complex dilaton fields. However non-geometric fluxes [163, 164] may give rise to such masses in a way quite similar to the Type IIA axions discussed above. In particular, in SUSY toroidal settings a superpotential term proportional to $W_{ng} = h_i T_i$ is created [163, 164]. This is mirror to the Type IIA one $W = h_i U_i$ which originates the mass term for the axions a_i above.

Let us close by noting that this axion state appearing in this class of string models is expected to come along with extra Z's which could also be detected at LHC [153, 154, 165, 166]. Indeed, there are 3 linear combinations of the $U(1)_{a,b,c,d}$'s which are orthogonal to hypercharge and become massive by combining with axions (or their 2-form duals) as

in eq. (3.4). There is in fact a 4×4 mass matrix for the U(1)'s given by [153]

$$(M^2)_{\alpha\beta} = \frac{M_s^2}{4\pi} g_\alpha g_\beta \sum_i c_i^\alpha c_i^\beta, \ \alpha, \beta = a, b, c, d, \qquad (3.18)$$

where g_α, g_β are the corresponding U(1) coupling constants, and the c_i^α are the integer coefficients appearing in eq. (3.4). This matrix has a zero eigenvalue $M_1 = 0$ corresponding to hypercharge. There are other three massive eigenvalues M_2, M_3, M_4. As pointed out in refs. [153, 154, 165, 166] in the toroidal setting described in the appendix [151] and others based on intersecting D5-branes [152], one eigenvalue is always above the string scale, but the other two are most often lighter, with one of them M_3 in the range $0.15 \, M_s \leq M_3 \leq 0.32 \, M_s$ [153]. So beyond a $750 \, \text{GeV}$ axion one could find at LHC an extra Z' of this class before reaching the string threshold. Present bounds on Z' from LHC stand around a region $1.5–3 \, \text{TeV}$ depending on the decay products [150, 167–169]. However it was shown in ref. [170] that Z's lighter than the maximum bound value for the mass of $3 \, \text{TeV}$ could evade those searches by a reduction of their couplings. So it could be that in the forthcoming LHC run such Z's in the $1.5\text{-}5 \, \text{TeV}$ region could be produced.

4 Conclusions

In the present paper we have analysed whether the hints for a $750 \, \text{GeV}$ resonance recently obtained by ATLAS and CMS experiments could be explained in terms of a heavy string axion in a scheme with low scale string theory. We have shown how in such models with a string scale $M_s \simeq 7\text{–}10^4 \, \text{TeV}$, there naturally appear massive pseudoscalar fields with axion-like couplings both to gluons and photons, but not to W's. We have exemplified this in the context of intersecting brane models in Type IIA orientifolds, in which the SM gauge bosons reside on D6-branes and quarks and leptons live at the intersection.

Interestingly, in the simplest toroidal examples there is a unique axion-like scalar a_0 with these properties, with all other axions in the theory becoming massive through a Green-Schwarz mechanism. We have shown how this axion has the correct couplings and a typical axion decay constant $f \simeq 10^{-2}\text{–}10^{-5} \, M_s$.

Standard axions are notorious for being perturbatively massless, due to their characteristic shift symmetry, and so it seems hard to understand how an axion field could get a mass as large as $750 \, \text{GeV}$. We show that the solution to this puzzle is automatic if the axion is a monodromy axion, of the type recently discussed in the context of string monodromy inflation [128–132] and, more recently, relaxion models [136, 137]. Monodromy axions may have a non-trivial scalar potential, and hence a mass, as long as not only the axion transforms under the discrete gauge shift symmetry $a_0 \to a_0 + 2\pi f$, but the potential parameters do. The structure is better described in terms of quantized Minkowski 4-forms [130, 131, 133]. In this paper we have shown how the axion a_0 in intersecting brane Type IIA models has the correct couplings and scalar potential of a monodromy axion in the presence of NS 3-form fluxes. This behaviour is not exceptional and we have also discussed how the same type of consisten axions and couplings arise in other string settings like large volume Type IIB orientifolds.

We have analysed the phenomenological prospects of such a heavy axion (we call it *megaxion*) in describing the hinted resonance at $750\,\mathrm{GeV}$. Describing the observed production and decay rates set constraints on the plane of axion couplings κ_g and κ_γ, figure (1). The requirement of an axion width of order $45\,\mathrm{GeV}$ as hinted by ATLAS, is not achieved in our scenario due to the dijet searches and the photon production. The allowed region implies values for the string axion decay width of $20\,\mathrm{GeV} \lesssim f/g_g \lesssim 10^3\,\mathrm{GeV}$ and $f/g_\gamma \simeq 25\,\mathrm{GeV}$, together with the region $2\,\mathrm{GeV} \lesssim f/g_\gamma \lesssim 25\,\mathrm{GeV}$ and $f/g_g \simeq 8\times10^2\,\mathrm{GeV}$, and the region $f/g_\gamma \simeq 2\,\mathrm{GeV}$ for values of κ_g greater than $\kappa_g \gtrsim 10^3\,\mathrm{GeV}$. If the preliminary experimental evidence is confirmed, these values will constraint specific low scale string models.

If the hint of a $750\,\mathrm{GeV}$ boson at LHC is confirmed, it would probably imply, in one way or the other, a revolution in our understanding of what lies beyond the Standard Model. We have explored here the possibility that this boson is identified with an axion-like state from a low scale string theory. This type of axion with the correct couplings and a large mass appears naturally in the context of string models with the SM living at intersecting branes. If that identification was correct, there would be good options to further observe at least some excess in the ZZ and $Z\gamma$ channels as well as one extra Z' at LHC before reaching the string threshold. We are looking forward to the analysis of the 2016 ATLAS and CMS data for a confirmation or not of this tantalising $750\,\mathrm{GeV}$ state.

Acknowledgments

A   The SM at intersecting D6-branes

The general structure of intersecting D6-brane models involve 4 sets of D6-branes in a Type IIA orientifold (see [144–149, 151]) There is a stack a) with 3 D6-branes carrying gauge group $\mathrm{U}(3)_a$, including QCD and a $\mathrm{U}(1)_a$; a stack b) with 2 branes and gauge group $\mathrm{U}(2)_b$, containing the EW $\mathrm{SU}(2)$ and a $\mathrm{U}(1)_b$; a stack c) with 1 brane, yielding a $\mathrm{U}(1)_c$ which is proportional to the Cartan generator of a (would be) gauge group $\mathrm{SU}(2)_R$ of left-right symmetric models; and a stack d) with gauge group $\mathrm{U}(1)_d$, which is proportional to the gauged lepton number. Being an orientifold, there is an orientifold Z_2 symmetry so that one has to include another set of 3+2+1+1 D6-branes denoted a^*, b^*, c^*, d^*, which are the orientifold mirrors of the former. The sets of D6-branes intersect at points in the 6 compact dimensions and at the intersection localised chiral fermions appear. The number of generations is given by the times a given pair of D6-branes intersect. The intersection numbers are chosen so that the obtained fermion spectrum is that of the SM. The chiral fermion spectrum and the charges of each of them under the 4 U(1)'s is shown in table (1)

Intersection	Matter fields		Q_a	Q_b	Q_c	Q_d	Y
(ab)	Q_L	$(3,2)$	1	-1	0	0	1/6
(ab*)	q_L	$2(3,2)$	1	1	0	0	1/6
(ac)	U_R	$3(\bar{3},1)$	-1	0	1	0	-2/3
(ac*)	D_R	$3(\bar{3},1)$	-1	0	-1	0	1/3
(bd*)	L	$3(1,2)$	0	-1	0	-1	-1/2
(cd)	E_R	$3(1,1)$	0	0	-1	1	1
(cd*)	N_R	$3(1,1)$	0	0	1	1	0

Table 1. Standard model spectrum and U(1) charges.

The hypercharge is given by the linear combination of U(1) charges

$$Q_Y = \frac{1}{6}Q_a - \frac{1}{2}Q_c + \frac{1}{2}Q_d .\qquad (A.1)$$

This general structure may be obtained for a variety of compact CY orientifold compactification. The simplest example is obtained in toroidal compactifications in which the 6 extra dimensions have a $T_1^2 \times T_2^2 \times T_3^2$ geometry, which is what we describe below. However one may also obtain this structure in more general conformal field theory orientifolds as in ref. [171].

Let us now briefly review the toroidal case. Each D6-brane contains Minkowski space and a 3-cycle volume Π_3 in compact dimensions. In these toroidal examples the 3-cycles are obtained by each D6 wrapping once each of the 3 T_i^2. In each torus T_i^2 each brane wraps n_i times along the x_i and m_i times around the y_i direction. Thus each 3-cycle is denoted by the set of 6 integers $(n_1,m_1)(n_2,m_2)(n_3,m_3)$. One can then check that the intersection number of two stacks of branes α,β is given by

$$I_{\alpha\beta} = \Pi_{i=1,2,3}(n_i^\alpha m_i^\beta - n_i^\beta m_i^\alpha) .\qquad (A.2)$$

It was shown in [151] that the most general choice of wrapping numbers (n_i, m_i) yielding just the chiral fermion content of the SM with three generations is given by those in table (2). In order to obtain the correct hypercharge massless U(1) those wrapping parameters have to verify the extra constraint

$$n_c^1 = \frac{\beta^2}{2\beta^1}(n_a^2 + 3\rho n_d^2) .\qquad (A.3)$$

In addition to the above SM sector there are also closed string moduli, complex structure and axionic fields. In particular, there are 4 axion fields η_i, $i = 0, 1, 2, 3$ from the RR sector

N_i	(n_i^1, m_i^1)	(n_i^2, m_i^2)	(n_i^3, m_i^3)
$N_a = 3$	$(1/\beta^1, 0)$	$(n_a^2, \epsilon\beta^2)$	$(1/\rho, 1/2)$
$N_b = 2$	$(n_b^1, -\epsilon\beta^1)$	$(1/\beta^2, 0)$	$(1, 3\rho/2)$
$N_c = 1$	$(n_c^1, 3\rho\epsilon\beta^1)$	$(1/\beta^2, 0)$	$(0, 1)$
$N_d = 1$	$(1/\beta^1, 0)$	$(n_d^2, -\beta^2\epsilon/\rho)$	$(1, 3\rho/2)$

Table 2. D6-brane wrapping numbers giving rise to a SM spectrum. The general solutions are parametrized by a phase $\epsilon = \pm 1$, the NS background on the first two tori $\beta^i = 1 - b^i = 1, 1/2$, four integers $n_a^2, n_b^1, n_c^1, n_d^2$ and a parameter $\rho = 1, 1/3$.

of the theory. Their dual 2-forms B_2^i have couplings to the U(1) field strengths given by

$$
\begin{aligned}
B_2^1 \ \wedge \ & \frac{-2\epsilon\beta^1}{\beta^2} F^b \\
B_2^2 \ \wedge \ & \frac{(\epsilon\beta^2)}{\rho\beta^1} \left(3F^a \ - \ F^d \right) \\
B_2^3 \ \wedge \ & \frac{1}{2\beta^2} \left(\frac{3\beta^2 n_a^2}{\beta^1} F^a \ + \ 6\rho n_b^1 F^b \ + \ 2n_c^1 F^c \ + \ \frac{3\rho\beta^2 n_d^2}{\beta^1} F^d \right)
\end{aligned}
\tag{A.4}
$$

whereas the B_2^0 RR field has no couplings to the F_j, because $\Pi_\alpha m_j^\alpha = 0$ for all the branes. Thus the axion η_0 remains massless, as mentioned in the main text. The dual scalars η^i have couplings:

$$
\begin{aligned}
\eta^1 \ & \left(\frac{\epsilon\beta^2}{2\beta^1} \right) \left(F^a \wedge F^a \ - \ 3F^d \wedge F^d \right) \\
\eta^2 \ & \left(\frac{3\rho\epsilon\beta^1}{2\beta^2} \right) \left(-F^b \wedge F^b \ + \ 2F^c \wedge F^c \right) \\
\eta^0 \ & \left(\frac{n_a^2}{\rho\beta^1} F^a \wedge F^a \ + \ \frac{n_b^1}{\beta^2} F^b \wedge F^b \ + \ \frac{n_d^2}{\beta^1} F^d \wedge F^d \right) .
\end{aligned}
\tag{A.5}
$$

The last equation here yields the coupling in eq. (3.5). In particular there is a large class of models with $n_b^1 = 0$ in which the axion η_0 does not couple to the W gauge bosons, as stated in the main text.

Let us finally mention that in this class of models, the proton is stable because baryon number is a gauged (though anomalous) gauge symmetry, which perturbatively forbids proton decay. Baryon number violation may only appear from gauge string instanton effects, which are generically exponentially suppressed.

References

[1] ATLAS collaboration, *Search for resonances decaying to photon pairs in 3.2 fb^{-1} of pp collisions at $\sqrt{s} = 13\,TeV$ with the ATLAS detector*, ATLAS-CONF-2015-081.

[2] CMS Collaboration, *Search for new physics in high mass diphoton events in proton-proton collisions at $\sqrt{s} = 13\,TeV$*, CMS-PAS-EXO-15-004.

[3] CMS Collaboration, *Search for new resonances in the diphoton final state in the range between 150 and 850 GeV in pp collisions at $\sqrt{s} = 8$ TeV*, CMS-PAS-HIG-14-006.

[4] ATLAS collaboration, *Search for high-mass diphoton resonances in pp collisions at $\sqrt{s} = 8\,TeV$ with the ATLAS detector*, *Phys. Rev.* **D 92** (2015) 032004 [arXiv:1504.05511] [INSPIRE].

[5] LHC Higgs Cross Section Working Group, https://twiki.cern.ch/twiki/bin/view/LHCPhysics/CrossSections.

[6] CMS collaboration, *Searches for new physics using the $t\bar{t}$ invariant mass distribution in pp collisions at $\sqrt{s} = 8\,TeV$*, *Phys. Rev. Lett.* **111** (2013) 211804 [arXiv:1309.2030] [INSPIRE].

[7] ATLAS collaboration, *Search for a high-mass Higgs boson decaying to a W boson pair in pp collisions at $\sqrt{s} = 8\,TeV$ with the ATLAS detector*, *JHEP* **01** (2016) 032 [arXiv:1509.00389] [INSPIRE].

[8] CMS collaboration, *Search for a Higgs Boson in the Mass Range from 145 to 1000 GeV Decaying to a Pair of W or Z Bosons*, *JHEP* **10** (2015) 144 [arXiv:1504.00936] [INSPIRE].

[9] ATLAS collaboration, *Search for an additional, heavy Higgs boson in the $H \to ZZ$ decay channel at $\sqrt{s} = 8\,TeV$ in pp collision data with the ATLAS detector*, *Eur. Phys. J.* **C 76** (2016) 45 [arXiv:1507.05930] [INSPIRE].

[10] ATLAS collaboration, *Search for new resonances in $W\gamma$ and $Z\gamma$ final states in pp collisions at $\sqrt{s} = 8\,TeV$ with the ATLAS detector*, *Phys. Lett.* **B 738** (2014) 428 [arXiv:1407.8150] [INSPIRE].

[11] ATLAS collaboration, *Search for high-mass dilepton resonances in pp collisions at $\sqrt{s} = 8$ TeV with the ATLAS detector*, *Phys. Rev.* **D 90** (2014) 052005 [arXiv:1405.4123] [INSPIRE].

[12] CMS collaboration, *Search for physics beyond the standard model in dilepton mass spectra in proton-proton collisions at $\sqrt{s} = 8\,TeV$*, *JHEP* **04** (2015) 025 [arXiv:1412.6302] [INSPIRE].

[13] CMS collaboration, *Search for neutral MSSM Higgs bosons decaying into a pair of bottom quarks*, *JHEP* **11** (2015) 071 [arXiv:1506.08329] [INSPIRE].

[14] J. Jaeckel, M. Jankowiak and M. Spannowsky, *LHC probes the hidden sector*, *Phys. Dark Univ.* **2** (2013) 111 [arXiv:1212.3620] [INSPIRE].

[15] K. Harigaya and Y. Nomura, *Composite Models for the 750 GeV Diphoton Excess*, *Phys. Lett.* **B 754** (2016) 151 [arXiv:1512.04850] [INSPIRE].

[16] Y. Mambrini, G. Arcadi and A. Djouadi, *The LHC diphoton resonance and dark matter*, *Phys. Lett.* **B 755** (2016) 426 [arXiv:1512.04913] [INSPIRE].

[17] M. Backovic, A. Mariotti and D. Redigolo, *Di-photon excess illuminates Dark Matter*, *JHEP* **03** (2016) 157 [arXiv:1512.04917] [INSPIRE].

[18] A. Angelescu, A. Djouadi and G. Moreau, *Scenarii for interpretations of the LHC diphoton excess: two Higgs doublets and vector-like quarks and leptons*, [*Phys. Lett.* **B 756** (2016) 126](#) [[arXiv:1512.04921](#)] [[INSPIRE](#)].

[19] Y. Nakai, R. Sato and K. Tobioka, *Footprints of New Strong Dynamics via Anomaly and the 750 GeV Diphoton*, [*Phys. Rev. Lett.* **116** (2016) 151802](#) [[arXiv:1512.04924](#)] [[INSPIRE](#)].

[20] S. Knapen, T. Melia, M. Papucci and K. Zurek, *Rays of light from the LHC*, [*Phys. Rev.* **D 93** (2016) 075020](#) [[arXiv:1512.04928](#)] [[INSPIRE](#)].

[21] D. Buttazzo, A. Greljo and D. Marzocca, *Knocking on new physics' door with a scalar resonance*, [*Eur. Phys. J.* **C 76** (2016) 116](#) [[arXiv:1512.04929](#)] [[INSPIRE](#)].

[22] A. Pilaftsis, *Diphoton Signatures from Heavy Axion Decays at the CERN Large Hadron Collider*, [*Phys. Rev.* **D 93** (2016) 015017](#) [[arXiv:1512.04931](#)] [[INSPIRE](#)].

[23] S. Di Chiara, L. Marzola and M. Raidal, *First interpretation of the 750 GeV diphoton resonance at the LHC*, [*Phys. Rev.* **D 93** (2016) 095018](#) [[arXiv:1512.04939](#)] [[INSPIRE](#)].

[24] T. Higaki, K.S. Jeong, N. Kitajima and F. Takahashi, *The QCD Axion from Aligned Axions and Diphoton Excess*, [*Phys. Lett.* **B 755** (2016) 13](#) [[arXiv:1512.05295](#)] [[INSPIRE](#)].

[25] S.D. McDermott, P. Meade and H. Ramani, *Singlet Scalar Resonances and the Diphoton Excess*, [*Phys. Lett.* **B 755** (2016) 353](#) [[arXiv:1512.05326](#)] [[INSPIRE](#)].

[26] J. Ellis, S.A.R. Ellis, J. Quevillon, V. Sanz and T. You, *On the Interpretation of a Possible ∼ 750 GeV Particle Decaying into γγ*, [*JHEP* **03** (2016) 176](#) [[arXiv:1512.05327](#)] [[INSPIRE](#)].

[27] M. Low, A. Tesi and L.-T. Wang, *A pseudoscalar decaying to photon pairs in the early LHC Run 2 data*, [*JHEP* **03** (2016) 108](#) [[arXiv:1512.05328](#)] [[INSPIRE](#)].

[28] B. Bellazzini, R. Franceschini, F. Sala and J. Serra, *Goldstones in Diphotons*, [*JHEP* **04** (2016) 072](#) [[arXiv:1512.05330](#)] [[INSPIRE](#)].

[29] R.S. Gupta, S. Jäger, Y. Kats, G. Perez and E. Stamou, *Interpreting a 750 GeV Diphoton Resonance*, [arXiv:1512.05332](#) [[INSPIRE](#)].

[30] C. Petersson and R. Torre, *750 GeV Diphoton Excess from the Goldstino Superpartner*, [*Phys. Rev. Lett.* **116** (2016) 151804](#) [[arXiv:1512.05333](#)] [[INSPIRE](#)].

[31] E. Molinaro, F. Sannino and N. Vignaroli, *Minimal Composite Dynamics versus Axion Origin of the Diphoton excess*, [arXiv:1512.05334](#) [[INSPIRE](#)].

[32] B. Dutta, Y. Gao, T. Ghosh, I. Gogoladze and T. Li, *Interpretation of the diphoton excess at CMS and ATLAS*, [*Phys. Rev.* **D 93** (2016) 055032](#) [[arXiv:1512.05439](#)] [[INSPIRE](#)].

[33] Q.-H. Cao, Y. Liu, K.-P. Xie, B. Yan and D.-M. Zhang, *A Boost Test of Anomalous Diphoton Resonance at the LHC*, [arXiv:1512.05542](#) [[INSPIRE](#)].

[34] S. Matsuzaki and K. Yamawaki, *750 GeV Diphoton Signal from One-Family Walking Technipion*, [*Mod. Phys. Lett.* **A 31** (2016) 1630016](#) [[arXiv:1512.05564](#)] [[INSPIRE](#)].

[35] A. Kobakhidze, F. Wang, L. Wu, J.M. Yang and M. Zhang, *750 GeV diphoton resonance in a top and bottom seesaw model*, [*Phys. Lett.* **B 757** (2016) 92](#) [[arXiv:1512.05585](#)] [[INSPIRE](#)].

[36] R. Martinez, F. Ochoa and C.F. Sierra, *Diphoton decay for a 750 GeV scalar boson in an* U(1)′ *model*, [arXiv:1512.05617](#) [[INSPIRE](#)].

[37] P. Cox, A.D. Medina, T.S. Ray and A. Spray, *Diphoton Excess at 750 GeV from a Radion in the Bulk-Higgs Scenario*, [arXiv:1512.05618](#) [[INSPIRE](#)].

[38] D. Bečirević, E. Bertuzzo, O. Sumensari and R. Zukanovich Funchal, *Can the new resonance at LHC be a CP-Odd Higgs boson?*, *Phys. Lett.* **B 757** (2016) 261 [arXiv:1512.05623] [INSPIRE].

[39] J.M. No, V. Sanz and J. Setford, *See-saw composite Higgs model at the LHC: Linking naturalness to the 750 GeV diphoton resonance*, *Phys. Rev.* **D 93** (2016) 095010 [arXiv:1512.05700] [INSPIRE].

[40] S.V. Demidov and D.S. Gorbunov, *On the sgoldstino interpretation of the diphoton excess*, *JETP Lett.* **103** (2016) 219 [arXiv:1512.05723] [INSPIRE].

[41] W. Chao, R. Huo and J.-H. Yu, *The Minimal Scalar-Stealth Top Interpretation of the Diphoton Excess*, arXiv:1512.05738 [INSPIRE].

[42] S. Fichet, G. von Gersdorff and C. Royon, *Scattering light by light at 750 GeV at the LHC*, *Phys. Rev.* **D 93** (2016) 075031 [arXiv:1512.05751] [INSPIRE].

[43] D. Curtin and C.B. Verhaaren, *Quirky Explanations for the Diphoton Excess*, *Phys. Rev.* **D 93** (2016) 055011 [arXiv:1512.05753] [INSPIRE].

[44] L. Bian, N. Chen, D. Liu and J. Shu, *Hidden confining world on the 750 GeV diphoton excess*, *Phys. Rev.* **D 93** (2016) 095011 [arXiv:1512.05759] [INSPIRE].

[45] J. Chakrabortty, A. Choudhury, P. Ghosh, S. Mondal and T. Srivastava, *Di-photon resonance around 750 GeV: shedding light on the theory underneath*, arXiv:1512.05767 [INSPIRE].

[46] A. Ahmed, B.M. Dillon, B. Grzadkowski, J.F. Gunion and Y. Jiang, *Higgs-radion interpretation of 750 GeV di-photon excess at the LHC*, arXiv:1512.05771 [INSPIRE].

[47] P. Agrawal, J. Fan, B. Heidenreich, M. Reece and M. Strassler, *Experimental Considerations Motivated by the Diphoton Excess at the LHC*, *JHEP* **06** (2016) 082 [arXiv:1512.05775] [INSPIRE].

[48] C. Csáki, J. Hubisz and J. Terning, *Minimal model of a diphoton resonance: Production without gluon couplings*, *Phys. Rev.* **D 93** (2016) 035002 [arXiv:1512.05776] [INSPIRE].

[49] A. Falkowski, O. Slone and T. Volansky, *Phenomenology of a 750 GeV Singlet*, *JHEP* **02** (2016) 152 [arXiv:1512.05777] [INSPIRE].

[50] D. Aloni, K. Blum, A. Dery, A. Efrati and Y. Nir, *On a possible large width 750 GeV diphoton resonance at ATLAS and CMS*, arXiv:1512.05778 [INSPIRE].

[51] Y. Bai, J. Berger and R. Lu, *750 GeV dark pion: Cousin of a dark G-parity odd WIMP*, *Phys. Rev.* **D 93** (2016) 076009 [arXiv:1512.05779] [INSPIRE].

[52] E. Gabrielli, K. Kannike, B. Mele, M. Raidal, C. Spethmann and H. Veermäe, *A SUSY Inspired Simplified Model for the 750 GeV Diphoton Excess*, *Phys. Lett.* **B 756** (2016) 36 [arXiv:1512.05961] [INSPIRE].

[53] R. Benbrik, C.-H. Chen and T. Nomura, *Higgs singlet boson as a diphoton resonance in a vectorlike quark model*, *Phys. Rev.* **D 93** (2016) 055034 [arXiv:1512.06028] [INSPIRE].

[54] J.S. Kim, J. Reuter, K. Rolbiecki and R. Ruiz de Austri, *A resonance without resonance: scrutinizing the diphoton excess at 750 GeV*, *Phys. Lett.* **B 755** (2016) 403 [arXiv:1512.06083] [INSPIRE].

[55] A. Alves, A.G. Dias and K. Sinha, *The 750 GeV S-cion: Where else should we look for it?*, *Phys. Lett.* **B 757** (2016) 39 [arXiv:1512.06091] [INSPIRE].

[56] E. Megias, O. Pujolàs and M. Quirós, *On dilatons and the LHC diphoton excess*, *JHEP* **05** (2016) 137 [arXiv:1512.06106] [InSPIRE].

[57] L.M. Carpenter, R. Colburn and J. Goodman, *Supersoft SUSY Models and the 750 GeV Diphoton Excess, Beyond Effective Operators*, arXiv:1512.06107 [InSPIRE].

[58] J. Bernon and C. Smith, *Could the width of the diphoton anomaly signal a three-body decay?*, *Phys. Lett.* **B 757** (2016) 148 [arXiv:1512.06113] [InSPIRE].

[59] W. Chao, *Symmetries behind the 750 GeV diphoton excess*, *Phys. Rev.* **D 93** (2016) 115013 [arXiv:1512.06297] [InSPIRE].

[60] M.T. Arun and P. Saha, *Gravitons in multiply warped scenarios — at 750 GeV and beyond*, arXiv:1512.06335 [InSPIRE].

[61] S. Chang, *A Simple* U(1) *Gauge Theory Explanation of the Diphoton Excess*, *Phys. Rev.* **D 93** (2016) 055016 [arXiv:1512.06426] [InSPIRE].

[62] H. Han, S. Wang and S. Zheng, *Scalar Explanation of Diphoton Excess at LHC*, *Nucl. Phys.* **B 907** (2016) 180 [arXiv:1512.06562] [InSPIRE].

[63] X.-F. Han and L. Wang, *Implication of the 750 GeV diphoton resonance on two-Higgs-doublet model and its extensions with Higgs field*, *Phys. Rev.* **D 93** (2016) 055027 [arXiv:1512.06587] [InSPIRE].

[64] D. Bardhan, D. Bhatia, A. Chakraborty, U. Maitra, S. Raychaudhuri and T. Samui, *Radion Candidate for the LHC Diphoton Resonance*, arXiv:1512.06674 [InSPIRE].

[65] W.S. Cho et al., *750 GeV Diphoton Excess May Not Imply a 750 GeV Resonance*, *Phys. Rev. Lett.* **116** (2016) 151805 [arXiv:1512.06824] [InSPIRE].

[66] J.M. Cline and Z. Liu, *LHC diphotons from electroweakly pair-produced composite pseudoscalars*, arXiv:1512.06827 [InSPIRE].

[67] M. Bauer and M. Neubert, *Flavor anomalies, the 750 GeV diphoton excess and a dark matter candidate*, *Phys. Rev.* **D 93** (2016) 115030 [arXiv:1512.06828] [InSPIRE].

[68] M. Chala, M. Duerr, F. Kahlhoefer and K. Schmidt-Hoberg, *Tricking Landau-Yang: How to obtain the diphoton excess from a vector resonance*, *Phys. Lett.* **B 755** (2016) 145 [arXiv:1512.06833] [InSPIRE].

[69] D. Barducci, A. Goudelis, S. Kulkarni and D. Sengupta, *One jet to rule them all: monojet constraints and invisible decays of a 750 GeV diphoton resonance*, *JHEP* **05** (2016) 154 [arXiv:1512.06842] [InSPIRE].

[70] O. Antipin, M. Mojaza and F. Sannino, *Minimal Coleman-Weinberg theory explains the diphoton excess*, *Phys. Rev.* **D 93** (2016) 115007 [arXiv:1512.06708] [InSPIRE].

[71] F. Wang, L. Wu, J.M. Yang and M. Zhang, *750 GeV diphoton resonance, 125 GeV Higgs and muon g — 2 anomaly in deflected anomaly mediation SUSY breaking scenarios*, *Phys. Lett.* **B 759** (2016) 191 [arXiv:1512.06715] [InSPIRE].

[72] J. Cao, C. Han, L. Shang, W. Su, J.M. Yang and Y. Zhang, *Interpreting the 750 GeV diphoton excess by the singlet extension of the Manohar-Wise model*, *Phys. Lett.* **B 755** (2016) 456 [arXiv:1512.06728] [InSPIRE].

[73] F.P. Huang, C.S. Li, Z.L. Liu and Y. Wang, *750 GeV Diphoton Excess from Cascade Decay*, arXiv:1512.06732 [InSPIRE].

[74] W. Liao and H.-q. Zheng, *Scalar resonance at 750 GeV as composite of heavy vector-like fermions*, arXiv:1512.06741 [INSPIRE].

[75] J.J. Heckman, *750 GeV Diphotons from a D3-brane*, *Nucl. Phys.* **B 906** (2016) 231 [arXiv:1512.06773] [INSPIRE].

[76] M. Dhuria and G. Goswami, *Perturbativity, vacuum stability and inflation in the light of 750 GeV diphoton excess*, arXiv:1512.06782 [INSPIRE].

[77] X.-J. Bi, Q.-F. Xiang, P.-F. Yin and Z.-H. Yu, *The 750 GeV diphoton excess at the LHC and dark matter constraints*, *Nucl. Phys.* **B 909** (2016) 43 [arXiv:1512.06787] [INSPIRE].

[78] J.S. Kim, K. Rolbiecki and R. Ruiz de Austri, *Model-independent combination of diphoton constraints at 750 GeV*, *Eur. Phys. J.* **C 76** (2016) 251 [arXiv:1512.06797] [INSPIRE].

[79] L. Berthier, J.M. Cline, W. Shepherd and M. Trott, *Effective interpretations of a diphoton excess*, *JHEP* **04** (2016) 084 [arXiv:1512.06799] [INSPIRE].

[80] S.M. Boucenna, S. Morisi and A. Vicente, *The LHC diphoton resonance from gauge symmetry*, *Phys. Rev.* **D 93** (2016) 115008 [arXiv:1512.06878] [INSPIRE].

[81] C.W. Murphy, *Vector Leptoquarks and the 750 GeV Diphoton Resonance at the LHC*, *Phys. Lett.* **B 757** (2016) 192 [arXiv:1512.06976] [INSPIRE].

[82] A.E.C. Hernández and I. Nisandzic, *LHC diphoton 750 GeV resonance as an indication of $SU(3)_c \times SU(3)_L \times U(1)_X$ gauge symmetry*, arXiv:1512.07165 [INSPIRE].

[83] U.K. Dey, S. Mohanty and G. Tomar, *750 GeV resonance in the dark left-right model*, *Phys. Lett.* **B 756** (2016) 384 [arXiv:1512.07212] [INSPIRE].

[84] G.M. Pelaggi, A. Strumia and E. Vigiani, *Trinification can explain the di-photon and di-boson LHC anomalies*, *JHEP* **03** (2016) 025 [arXiv:1512.07225] [INSPIRE].

[85] J. de Blas, J. Santiago and R. Vega-Morales, *New vector bosons and the diphoton excess*, *Phys. Lett.* **B 759** (2016) 247 [arXiv:1512.07229] [INSPIRE].

[86] A. Belyaev, G. Cacciapaglia, H. Cai, T. Flacke, A. Parolini and H. Serôdio, *Singlets in Composite Higgs Models in light of the LHC di-photon searches*, arXiv:1512.07242 [INSPIRE].

[87] P.S.B. Dev and D. Teresi, *Asymmetric Dark Matter in the Sun and the Diphoton Excess at the LHC*, arXiv:1512.07243 [INSPIRE].

[88] W.-C. Huang, Y.-L.S. Tsai and T.-C. Yuan, *Gauged Two Higgs Doublet Model confronts the LHC 750 GeV diphoton anomaly*, *Nucl. Phys.* **B 909** (2016) 122 [arXiv:1512.07268] [INSPIRE].

[89] S. Moretti and K. Yagyu, *750 GeV diphoton excess and its explanation in two-Higgs-doublet models with a real inert scalar multiplet*, *Phys. Rev.* **D 93** (2016) 055043 [arXiv:1512.07462] [INSPIRE].

[90] K.M. Patel and P. Sharma, *Interpreting 750 GeV diphoton excess in SU(5) grand unified theory*, *Phys. Lett.* **B 757** (2016) 282 [arXiv:1512.07468] [INSPIRE].

[91] M. Badziak, *Interpreting the 750 GeV diphoton excess in minimal extensions of Two-Higgs-Doublet models*, *Phys. Lett.* **B 759** (2016) 464 [arXiv:1512.07497] [INSPIRE].

[92] S. Chakraborty, A. Chakraborty and S. Raychaudhuri, *Diphoton resonance at 750 GeV in the broken MRSSM*, arXiv:1512.07527 [INSPIRE].

[93] Q.-H. Cao, S.-L. Chen and P.-H. Gu, *Strong CP Problem, Neutrino Masses and the 750 GeV Diphoton Resonance*, arXiv:1512.07541 [INSPIRE].

[94] W. Altmannshofer, J. Galloway, S. Gori, A.L. Kagan, A. Martin and J. Zupan, *750 GeV diphoton excess*, *Phys. Rev.* **D 93** (2016) 095015 [arXiv:1512.07616] [INSPIRE].

[95] J. Gu and Z. Liu, *Physics implications of the diphoton excess from the perspective of renormalization group flow*, *Phys. Rev.* **D 93** (2016) 075006 [arXiv:1512.07624] [INSPIRE].

[96] B.C. Allanach, P.S.B. Dev, S.A. Renner and K. Sakurai, *750 GeV diphoton excess explained by a resonant sneutrino in R-parity violating supersymmetry*, *Phys. Rev.* **D 93** (2016) 115022 [arXiv:1512.07645] [INSPIRE].

[97] H. Davoudiasl and C. Zhang, *750 GeV messenger of dark conformal symmetry breaking*, *Phys. Rev.* **D 93** (2016) 055006 [arXiv:1512.07672] [INSPIRE].

[98] N. Craig, P. Draper, C. Kilic and S. Thomas, *Shedding Light on Diphoton Resonances*, *Phys. Rev.* **D 93** (2016) 115023 [arXiv:1512.07733] [INSPIRE].

[99] K. Das and S.K. Rai, *750 GeV diphoton excess in a* U(1) *hidden symmetry model*, *Phys. Rev.* **D 93** (2016) 095007 [arXiv:1512.07789] [INSPIRE].

[100] K. Cheung, P. Ko, J.S. Lee, J. Park and P.-Y. Tseng, *A Higgcision study on the 750 GeV Di-photon Resonance and 125 GeV SM Higgs boson with the Higgs-Singlet Mixing*, arXiv:1512.07853 [INSPIRE].

[101] J. Liu, X.-P. Wang and W. Xue, *LHC diphoton excess from colorful resonances*, arXiv:1512.07885 [INSPIRE].

[102] J. Zhang and S. Zhou, *Electroweak Vacuum Stability and Diphoton Excess at 750 GeV*, *Chin. Phys.* **C 40** (2016) 081001 [arXiv:1512.07889] [INSPIRE].

[103] J.A. Casas, J.R. Espinosa and J.M. Moreno, *The 750 GeV Diphoton Excess as a First Light on Supersymmetry Breaking*, *Phys. Lett.* **B 759** (2016) 159 [arXiv:1512.07895] [INSPIRE].

[104] L.J. Hall, K. Harigaya and Y. Nomura, *750 GeV Diphotons: Implications for Supersymmetric Unification*, *JHEP* **03** (2016) 017 [arXiv:1512.07904] [INSPIRE].

[105] H. Han, S. Wang and S. Zheng, *Dark Matter Theories in the Light of Diphoton Excess*, arXiv:1512.07992 [INSPIRE].

[106] J.-C. Park and S.C. Park, *Indirect signature of dark matter with the diphoton resonance at 750 GeV*, arXiv:1512.08117 [INSPIRE].

[107] A. Salvio and A. Mazumdar, *Higgs Stability and the 750 GeV Diphoton Excess*, *Phys. Lett.* **B 755** (2016) 469 [arXiv:1512.08184] [INSPIRE].

[108] D. Chway, R. Dermíšek, T.H. Jung and H.D. Kim, *Glue to light signal of a new particle*, arXiv:1512.08221 [INSPIRE].

[109] G. Li, Y.-n. Mao, Y.-L. Tang, C. Zhang, Y. Zhou and S.-h. Zhu, *Pseudoscalar Decaying Only via Loops as an Explanation for the 750 GeV Diphoton Excess*, *Phys. Rev. Lett.* **116** (2016) 151803 [arXiv:1512.08255] [INSPIRE].

[110] M. Son and A. Urbano, *A new scalar resonance at 750 GeV: Towards a proof of concept in favor of strongly interacting theories*, *JHEP* **05** (2016) 181 [arXiv:1512.08307] [INSPIRE].

[111] Y.-L. Tang and S.-h. Zhu, *NMSSM extended with vector-like particles and the diphoton excess on the LHC*, arXiv:1512.08323 [INSPIRE].

[112] H. An, C. Cheung and Y. Zhang, *Broad Diphotons from Narrow States*, arXiv:1512.08378 [INSPIRE].

[113] J. Cao, L. Shang, W. Su, F. Wang and Y. Zhang, *Interpreting The 750 GeV Diphoton Excess Within Topflavor Seesaw Model*, arXiv:1512.08392 [INSPIRE].

[114] F. Wang, W. Wang, L. Wu, J.M. Yang and M. Zhang, *Interpreting 750 GeV diphoton resonance as degenerate Higgs bosons in NMSSM with vector-like particles*, arXiv:1512.08434 [INSPIRE].

[115] C. Cai, Z.-H. Yu and H.-H. Zhang, *750 GeV diphoton resonance as a singlet scalar in an extra dimensional model*, *Phys. Rev.* **D 93** (2016) 075033 [arXiv:1512.08440] [INSPIRE].

[116] Q.-H. Cao, Y. Liu, K.-P. Xie, B. Yan and D.-M. Zhang, *Diphoton excess, low energy theorem and the 331 model*, *Phys. Rev.* **D 93** (2016) 075030 [arXiv:1512.08441] [INSPIRE].

[117] J.E. Kim, *Is an axizilla possible for di-photon resonance?*, *Phys. Lett.* **B 755** (2016) 190 [arXiv:1512.08467] [INSPIRE].

[118] J. Gao, H. Zhang and H.X. Zhu, *Diphoton excess at 750 GeV: gluon-gluon fusion or quark-antiquark annihilation?*, *Eur. Phys. J.* **C 76** (2016) 348 [arXiv:1512.08478] [INSPIRE].

[119] W. Chao, *Neutrino Catalyzed Diphoton Excess*, arXiv:1512.08484 [INSPIRE].

[120] X.-J. Bi, R. Ding, Y. Fan, L. Huang, C. Li, T. Li et al., *A Promising Interpretation of Diphoton Resonance at 750 GeV*, arXiv:1512.08497 [INSPIRE].

[121] F. Goertz, J.F. Kamenik, A. Katz and M. Nardecchia, *Indirect Constraints on the Scalar Di-Photon Resonance at the LHC*, *JHEP* **05** (2016) 187 [arXiv:1512.08500] [INSPIRE].

[122] P.S.B. Dev, R.N. Mohapatra and Y. Zhang, *Quark Seesaw, Vectorlike Fermions and Diphoton Excess*, *JHEP* **02** (2016) 186 [arXiv:1512.08507] [INSPIRE].

[123] N. Bizot, S. Davidson, M. Frigerio and J.L. Kneur, *Two Higgs doublets to explain the excesses* $pp \to \gamma\gamma(750\,GeV)$ *and* $h \to \tau^{\pm}\mu^{\mp}$, *JHEP* **03** (2016) 073 [arXiv:1512.08508] [INSPIRE].

[124] Y. Hamada, T. Noumi, S. Sun and G. Shiu, *An O(750) GeV Resonance and Inflation*, *Phys. Rev.* **D 93** (2016) 123514 [arXiv:1512.08984] [INSPIRE].

[125] R. Franceschini et al., *What is the* $\gamma\gamma$ *resonance at 750 GeV?*, *JHEP* **03** (2016) 144 [arXiv:1512.04933] [INSPIRE].

[126] M. Cvetič, J. Halverson and P. Langacker, *String Consistency, Heavy Exotics and the 750 GeV Diphoton Excess at the LHC*, arXiv:1512.07622 [INSPIRE].

[127] L.A. Anchordoqui, I. Antoniadis, H. Goldberg, X. Huang, D. Lüst and T.R. Taylor, *750 GeV diphotons from closed string states*, *Phys. Lett.* **B 755** (2016) 312 [arXiv:1512.08502] [INSPIRE].

[128] E. Silverstein and A. Westphal, *Monodromy in the CMB: Gravity Waves and String Inflation*, *Phys. Rev.* **D 78** (2008) 106003 [arXiv:0803.3085] [INSPIRE].

[129] L. McAllister, E. Silverstein and A. Westphal, *Gravity Waves and Linear Inflation from Axion Monodromy*, *Phys. Rev.* **D 82** (2010) 046003 [arXiv:0808.0706] [INSPIRE].

[130] N. Kaloper and L. Sorbo, *A Natural Framework for Chaotic Inflation*, *Phys. Rev. Lett.* **102** (2009) 121301 [arXiv:0811.1989] [INSPIRE].

[131] N. Kaloper, A. Lawrence and L. Sorbo, *An Ignoble Approach to Large Field Inflation*, *JCAP* **03** (2011) 023 [arXiv:1101.0026] [ɪɴSPIRE].

[132] F. Marchesano, G. Shiu and A.M. Uranga, *F-term Axion Monodromy Inflation*, *JHEP* **09** (2014) 184 [arXiv:1404.3040] [ɪɴSPIRE].

[133] S. Bielleman, L.E. Ibáñez and I. Valenzuela, *Minkowski 3-forms, Flux String Vacua, Axion Stability and Naturalness*, *JHEP* **12** (2015) 119 [arXiv:1507.06793] [ɪɴSPIRE].

[134] R. Bousso and J. Polchinski, *Quantization of four form fluxes and dynamical neutralization of the cosmological constant*, *JHEP* **06** (2000) 006 [hep-th/0004134] [ɪɴSPIRE].

[135] J.L. Feng, J. March-Russell, S. Sethi and F. Wilczek, *Saltatory relaxation of the cosmological constant*, *Nucl. Phys.* **B 602** (2001) 307 [hep-th/0005276] [ɪɴSPIRE].

[136] L.E. Ibáñez, M. Montero, A. Uranga and I. Valenzuela, *Relaxion Monodromy and the Weak Gravity Conjecture*, *JHEP* **04** (2016) 020 [arXiv:1512.00025] [ɪɴSPIRE].

[137] A. Hebecker, J. Moritz, A. Westphal and L.T. Witkowski, *Axion Monodromy Inflation with Warped KK-Modes*, *Phys. Lett.* **B 754** (2016) 328 [arXiv:1512.04463] [ɪɴSPIRE].

[138] ATLAS collaboration, *Search for new phenomena in the dijet mass distribution using $p - p$ collision data at $\sqrt{s} = 8\,TeV$ with the ATLAS detector*, *Phys. Rev.* **D 91** (2015) 052007 [arXiv:1407.1376] [ɪɴSPIRE].

[139] CMS Collaboration, *Search for Resonances Decaying to Dijet Final States at $\sqrt{s} = 8\,TeV$ with Scouting Data*, CMS-PAS-EXO-14-005.

[140] S. Fichet, G. von Gersdorff and C. Royon, *Scattering light by light at $750\,GeV$ at the LHC*, *Phys. Rev.* **D 93** (2016) 075031 [arXiv:1512.05751] [ɪɴSPIRE].

[141] C. Csáki, J. Hubisz and J. Terning, *Minimal model of a diphoton resonance: Production without gluon couplings*, *Phys. Rev.* **D 93** (2016) 035002 [arXiv:1512.05776] [ɪɴSPIRE].

[142] C. Csáki, J. Hubisz, S. Lombardo and J. Terning, *Gluon versus photon production of a $750\,GeV$ diphoton resonance*, *Phys. Rev.* **D 93** (2016) 095020 [arXiv:1601.00638] [ɪɴSPIRE].

[143] I. Antoniadis, N. Arkani-Hamed, S. Dimopoulos and G.R. Dvali, *New dimensions at a millimeter to a Fermi and superstrings at a TeV*, *Phys. Lett.* **B 436** (1998) 257 [hep-ph/9804398] [ɪɴSPIRE].

[144] L.E. Ibáñez and A. Uranga, *String Theory and Particle Physics. An Introduction to String Phenomenology*, Cambridge University Press, Cambridge U.K. (2012).

[145] F. Marchesano, *Progress in D-brane model building*, *Fortsch. Phys.* **55** (2007) 491 [hep-th/0702094] [ɪɴSPIRE].

[146] A.M. Uranga, *Chiral four-dimensional string compactifications with intersecting D-branes*, *Class. Quant. Grav.* **20** (2003) S373 [hep-th/0301032] [ɪɴSPIRE].

[147] R. Blumenhagen, M. Cvetič, P. Langacker and G. Shiu, *Toward realistic intersecting D-brane models*, *Ann. Rev. Nucl. Part. Sci.* **55** (2005) 71 [hep-th/0502005] [ɪɴSPIRE].

[148] F.G. Marchesano Buznego, *Intersecting D-brane models*, hep-th/0307252 [ɪɴSPIRE].

[149] D. Cremades, L.E. Ibáñez and F. Marchesano, *More about the standard model at intersecting branes*, hep-ph/0212048 [ɪɴSPIRE].

[150] CMS collaboration, *Search for narrow resonances decaying to dijets in proton-proton collisions at* $\sqrt{s} = 13\,TeV$, *Phys. Rev. Lett.* **116** (2016) 071801 [`arXiv:1512.01224`] [ɪɴSPIRE].

[151] L.E. Ibáñez, F. Marchesano and R. Rabadán, *Getting just the standard model at intersecting branes*, *JHEP* **11** (2001) 002 [`hep-th/0105155`] [ɪɴSPIRE].

[152] D. Cremades, L.E. Ibáñez and F. Marchesano, *Standard model at intersecting D5-branes: Lowering the string scale*, *Nucl. Phys.* **B 643** (2002) 93 [`hep-th/0205074`] [ɪɴSPIRE].

[153] D.M. Ghilencea, L.E. Ibáñez, N. Irges and F. Quevedo, *TeV scale Z-prime bosons from D-branes*, *JHEP* **08** (2002) 016 [`hep-ph/0205083`] [ɪɴSPIRE].

[154] D.M. Ghilencea, U(1) *masses in intersecting D-brane SM-like models*, *Nucl. Phys.* **B 648** (2003) 215 [`hep-ph/0208205`] [ɪɴSPIRE].

[155] T.W. Grimm and J. Louis, *The Effective action of type IIA Calabi-Yau orientifolds*, *Nucl. Phys.* **B 718** (2005) 153 [`hep-th/0412277`] [ɪɴSPIRE].

[156] J. Louis and A. Micu, *Type 2 theories compactified on Calabi-Yau threefolds in the presence of background fluxes*, *Nucl. Phys.* **B 635** (2002) 395 [`hep-th/0202168`] [ɪɴSPIRE].

[157] G. Villadoro and F. Zwirner, $N = 1$ *effective potential from dual type-IIA D6/O6 orientifolds with general fluxes*, *JHEP* **06** (2005) 047 [`hep-th/0503169`] [ɪɴSPIRE].

[158] O. DeWolfe, A. Giryavets, S. Kachru and W. Taylor, *Type IIA moduli stabilization*, *JHEP* **07** (2005) 066 [`hep-th/0505160`] [ɪɴSPIRE].

[159] P.G. Camara, A. Font and L.E. Ibáñez, *Fluxes, moduli fixing and MSSM-like vacua in a simple IIA orientifold*, *JHEP* **09** (2005) 013 [`hep-th/0506066`] [ɪɴSPIRE].

[160] V. Balasubramanian, P. Berglund, J.P. Conlon and F. Quevedo, *Systematics of moduli stabilisation in Calabi-Yau flux compactifications*, *JHEP* **03** (2005) 007 [`hep-th/0502058`] [ɪɴSPIRE].

[161] J.P. Conlon, F. Quevedo and K. Suruliz, *Large-volume flux compactifications: Moduli spectrum and D3/D7 soft supersymmetry breaking*, *JHEP* **08** (2005) 007 [`hep-th/0505076`] [ɪɴSPIRE].

[162] A. Maharana and E. Palti, *Models of Particle Physics from Type IIB String Theory and F-theory: A Review*, *Int. J. Mod. Phys.* **A 28** (2013) 1330005 [`arXiv:1212.0555`] [ɪɴSPIRE].

[163] J. Shelton, W. Taylor and B. Wecht, *Nongeometric flux compactifications*, *JHEP* **10** (2005) 085 [`hep-th/0508133`] [ɪɴSPIRE].

[164] G. Aldazabal, P.G. Camara, A. Font and L.E. Ibáñez, *More dual fluxes and moduli fixing*, *JHEP* **05** (2006) 070 [`hep-th/0602089`] [ɪɴSPIRE].

[165] L.A. Anchordoqui et al., *LHC Phenomenology and Cosmology of String-Inspired Intersecting D-brane Models*, *Phys. Rev.* **D 86** (2012) 066004 [`arXiv:1206.2537`] [ɪɴSPIRE].

[166] L.A. Anchordoqui, I. Antoniadis, H. Goldberg, X. Huang, D. Lüst and T.R. Taylor, *Stringy origin of diboson and dijet excesses at the LHC*, *Phys. Lett.* **B 749** (2015) 484 [`arXiv:1507.05299`] [ɪɴSPIRE].

[167] ATLAS collaboration, *Search for new phenomena in dijet mass and angular distributions from pp collisions at* $\sqrt{s} = 13\,TeV$ *with the ATLAS detector*, *Phys. Lett.* **B 754** (2016) 302 [`arXiv:1512.01530`] [ɪɴSPIRE].

[168] ATLAS collaboration, *Search for new phenomena in the dilepton final state using proton-proton collisions at $\sqrt{s} = 13\,TeV$ with the ATLAS detector*, ATLAS-CONF-2015-070.

[169] CMS Collaboration, *Search for a Narrow Resonance Produced in 13 TeV pp Collisions Decaying to Electron Pair or Muon Pair Final States*, CMS-PAS-EXO-15-005.

[170] V.M. Lozano, M. Peiró and P. Soler, *Isospin violating dark matter in Stückelberg portal scenarios*, *JHEP* **04** (2015) 175 [arXiv:1503.01780] [INSPIRE].

[171] T.P.T. Dijkstra, L.R. Huiszoon and A.N. Schellekens, *Supersymmetric standard model spectra from RCFT orientifolds*, *Nucl. Phys.* **B 710** (2005) 3 [hep-th/0411129] [INSPIRE].